Anisotropic Eliashberg theory for superconductivity in compressed and doped MgB_2

Hyoung Joon Choi,[1,*] Steven G. Louie,[2,3] and Marvin L. Cohen[2,3]
[1]*Department of Physics and IPAP, Yonsei University, Seoul 120-749, Korea*
[2]*Department of Physics, University of California at Berkeley, Berkeley, California 94720, USA*
[3]*Materials Sciences Division, Lawrence Berkeley National Laboratory, Berkeley, California 94720, USA*
(Received 21 July 2008; revised manuscript received 31 January 2009; published 18 March 2009)

We have studied superconducting properties of compressed and doped MgB_2 by performing first-principles calculations of the normal material properties and by solving the fully anisotropic Eliashberg equations. At each pressure or doping, electronic structures, phonon spectra, and momentum-dependent electron-phonon coupling strengths are calculated. Then using the fully anisotropic Eliashberg equations, the superconducting transition temperatures (T_c), the superconducting energy gaps [$\Delta(\vec{k})$], and the specific heats are obtained. Our results show that the multiple-gap nature of $\Delta(\vec{k})$ in MgB_2 is robust with applied pressure although T_c and $\Delta(\vec{k})$ decrease substantially and that electron doping reduces T_c and degrades severely the superconducting energy gap in the π bands.

DOI: 10.1103/PhysRevB.79.094518 PACS number(s): 74.70.Ad, 74.20.−z, 71.15.Mb

The compound MgB_2 is a phonon-mediated superconductor with a remarkable superconducting transition temperature T_c which can be as high as 40 K.[1–4] Since the first discovery, the effects of pressure and doping on its superconducting properties have been studied extensively in order to obtain more information about its superconductivity and to search for interesting changes in the superconducting properties such as higher T_c.[5]

Measurements of T_c of compressed MgB_2 have been widely performed and reported values of dT_c/dP ranging from −0.35 to −2 K/GPa.[5–10] A relatively weak pressure dependence was observed by Monteverde *et al.*[6] and their data, showing $dT_c/dP \approx -0.7$ K/GPa on average from 0 to 25 GPa, were analyzed either with a linear plus quadratic dependence having initial slope of −0.35 K/GPa or with a linear dependence of −0.8 K/GPa depending on the samples.[6] While a much stronger dependence of $dT_c/dP = -2.0$ K/GPa is also observed,[7–9] the values around −1.1 K/GPa are often measured in experiments using helium as the pressure medium.[10,11] It has been suggested that the variation in reported values of dT_c/dP may result primarily from shear-stress effects in nonhydrostatic pressure media rather than from the differences in the samples and that −1.1 K/GPa is the intrinsic value of the material under hydrostatic pressure.[10]

A key factor determining dT_c/dP is the frequency change $d\omega/dP$ of B-B bond-stretching modes (E_{2g} modes) that mediate the strong attractive interaction between holes in the boron σ bands. The E_{2g} modes are Raman active and are observed to produce anomalous one- or two-peak feature in Raman spectra with pressure from 0 to 15 GPa.[12–14] In the case of Raman measurements showing a one-peak feature,[12] a very broad peak near 620 cm^{-1} at 0 GPa moves to 790 cm^{-1} at 15 GPa resulting in very large mode-Grüneisen parameter $\gamma = d \ln \omega / 3d \ln a = 3.9 \pm 0.4$. Here a is the in-plane lattice constant. On the other hand, in the case of Raman spectra showing two-peak features,[13,14] the overall shape of the spectra changes with pressure. As pressure increases, the broad peak near 620 cm^{-1} becomes gradually weaker in intensity, being shifted quite slowly to higher energy, and a new peak develops at much higher energy.[13,14] In this case, the value of γ could be almost the same as that in the former case if one would estimate γ from the lower-energy peak position at 0 GPa and the higher-energy one at 15 GPa.[13,14] Thus, it has been discussed that the two Raman measurements may observe essentially the same feature, that is, the two-peak feature, but with different broadening of the Raman signal.[13]

Doping effects have been studied mainly with Al- or C-doped samples. With Al doping, the unit-cell volume decreases,[15–17] the Raman spectra show two-peak features,[18] and T_c decreases.[15–20] The superconducting energy gaps Δ_σ and Δ_π in Al-doped samples are measured by specific-heat measurements[15,21] and by point-contact measurements.[19] Carbon doping produces similar effects as Al doping. With C doping, the unit cell shrinks,[22,23] T_c decreases,[19,22–27] and the peak in Raman spectra is shifted substantially.[27] The superconducting energy gaps Δ_σ and Δ_π in C-doped samples are measured by point-contact measurements[19,25] and by angle-resolve photoemission spectroscopy.[26]

Previous theoretical studies of compressed or doped MgB_2 are based on the McMillan formula[14,28–31] and two-band Eliashberg equations.[32–34] The change of T_c with pressure is estimated to be $d \ln T_c/dP \approx -0.036$/GPa by using McMillan formula with assumed $\lambda = 0.7$ and $\mu^* = 0.1$,[28] claiming that the increase in the characteristic phonon frequency is the dominant contribution to the decrease of T_c under pressure.[14,28] A more rigorous study of the pressure effect on T_c is performed using two-band Eliashberg equations with scaled $\alpha^2 F_{ij}(\omega)$.[33] Doping effects are also studied using McMillan formula[30] and the two-band Eliashberg equations with $\alpha^2 F_{ij}(\omega)$ scaled by the electronic density of states at the Fermi level [$N(E_F)$] and the E_{2g} phonon frequencies.[32,34] For the multiple-gap nature of the superconductivity in MgB_2, anisotropic Eliashberg equations are more appropriate for analyzing or predicting the pressure or doping effect on T_c; but the McMillan formula is widely used because of its simplicity. At this point, none of the previous theoretical work is based on the fully anisotropic Eliashberg equations except for a few based on two-band Eliashberg equations with scaled $\alpha^2 F_{ij}(\omega)$.

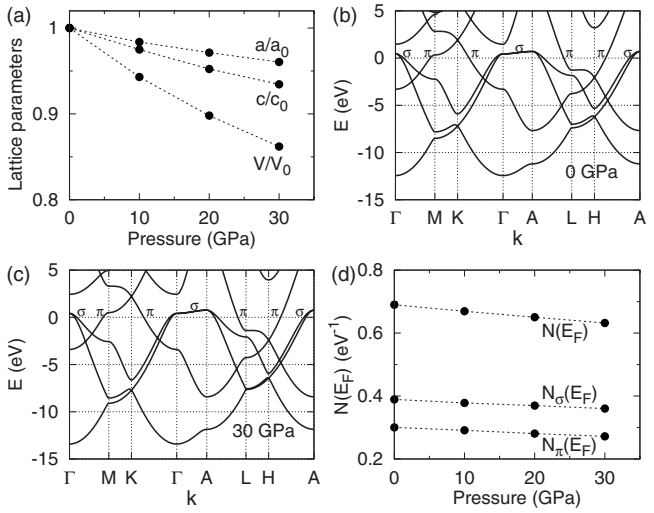

FIG. 1. Calculated lattice constants and electronic structures of compressed MgB_2: (a) lattice parameters and cell volume, (b) electronic band structure at 0 GPa, (c) electronic band structure at 30 GPa, and (d) the density of states at the Fermi level in states/eV/unit cell. In (a), the lattice parameters and unit-cell volume at 0 GPa are a_0, c_0, and V_0, respectively. In (d), the total density of states at the Fermi level is $N(E_F)$, and $N_\sigma(E_F)$ and $N_\pi(E_F)$ are the densities of states of the σ and π bands, respectively.

In this paper, we report on theoretical determinations of the superconducting properties of compressed and doped MgB_2 obtained using fully anisotropic Eliashberg equations[35,36] constructed on the basis of first-principles calculations.[37–40] We obtain electronic structures, phonon dispersions, and electron-phonon interaction for each pressure or doping and calculate T_c, the superconducting energy gap $\Delta(\vec{k})$, and the specific heat as functions of temperature. Our results show that the two-gap nature of the superconductivity persists when pressure is applied and that the electron doping strongly reduces the superconducting energy gap on the Fermi surface of the π bands.

We perform *ab initio* pseudopotential density-functional calculations to obtain lattice parameters, electronic structures, and phonon frequencies under pressure or doping.[37–40] *Ab initio* norm-conserving pseudopotentials[37] are used to describe the ionic potentials of boron and magnesium, and the local-density approximation (LDA) is applied to calculate the exchange and correlation energies, using plane waves of up to 60 Ry for the wave-function expansion. We use a $12\times12\times12$ k-point grid in the Brillouin zone (BZ) for self-consistent calculations and then used a $18\times18\times12$ grid and the linear tetrahedron method for the Fermi-surface properties.

To study the effect of pressure, we first calculate the lattice parameters of MgB_2 under pressure up to 30 GPa. Equilibrium lattice constants are calculated by relaxing the stress on the lattice except for applied hydrostatic pressure. The lattice parameters obtained show a monotonic decrease, as shown in Fig. 1(a) and Table I. At 30 GPa, the lattice constants a and c and the unit-cell volume V are decreased by 4.0%, 6.6%, and 14%, respectively. These results agree well with experimental results[41,42] and previous theoretical results.[42]

TABLE I. Calculated lattice parameters, cell volumes, density of states at the Fermi level, phonon frequencies, T_c's, and superconducting energy gaps Δ of compressed MgB_2. The total density of states at the Fermi level is $N(E_F)$, and $N_\sigma(E_F)$ and $N_\pi(E_F)$ are the densities of states of the σ and π bands, respectively. The harmonic and anharmonic frequencies of E_{2g} modes at Γ are ω_h and ω_a, respectively, and Δ_σ and Δ_π are the average values of $\Delta(\vec{k})$ on the σ and π Fermi surfaces at low temperature, respectively.

Pressure	0 GPa	10 GPa	20 GPa	30 GPa
a (Å)	3.07	3.02	2.98	2.95
c (Å)	3.57	3.48	3.40	3.34
V (Å^3)	29.2	27.6	26.3	25.2
$N_\sigma(E_F)$	0.30	0.29	0.28	0.27
$N_\pi(E_F)$	0.39	0.38	0.37	0.36
$N(E_F)$	0.69	0.67	0.65	0.63
ω_h (meV)	63.7	74.5	82.3	89.2
ω_h (cm^{-1})	506	601	664	720
ω_a (meV)	75.9	83.7	90.7	96.7
ω_a (cm^{-1})	612	675	732	780
T_c (K)	39	33	28	24
Δ_σ (meV)	6.7	5.4	4.5	3.9
Δ_π (meV)	1.8	1.3	1.03	0.85
$2\Delta_\sigma/k_BT_c$	4.0	3.9	3.8	3.8
$2\Delta_\pi/k_BT_c$	1.1	0.93	0.86	0.83

As the volume decreases with applied pressure, the overall bandwidth increases [Figs. 1(b) and 1(c)] and the density of states at the Fermi level $N(E_F)$ decreases [Fig. 1(d) and Table I]. At 30 GPa, $N(E_F)$ is reduced by 8.4% (Table I), in good agreement with previous theoretical results.[28] When $N(E_F)$ is decomposed into the densities of states of the σ and π bands [$N_\sigma(E_F)$ and $N_\pi(E_F)$], the former decreases slightly faster than the latter [Fig. 1(d) and Table I].

The phonon frequencies are calculated at high-symmetry points by a frozen-phonon method and then their dispersions in the full BZ are obtained by interpolating the dynamical matrix. Phonon anharmonicity is extracted from the frozen-phonon calculations and then used in the frequency calculations.[3] Matrix elements for electron-phonon coupling are obtained for phonons at the high-symmetry points and then they are interpolated in the full BZ.

Figure 2 shows the calculated phonon dispersions at various pressures. Anharmonicity is included in the dispersions by the method described in detail in Ref. 3. Compared with corresponding values at 0 GPa, frequencies at 30 GPa of the E_{1u}, A_{2u}, E_{2g}, and B_{1g} modes at Γ are increased by 30%, 32%, 27%, and 11%, respectively. We note that at 30 GPa, the frequencies of the E_{2g} modes are even higher than those of the B_{1g} mode [Fig. 2(c)]. In particular, the rate of frequency change of the E_{2g} modes at Γ is $d(\hbar\omega_a)/dP = 0.70$ meV/GPa or equivalently $d\ln(\hbar\omega_a)/dP = 0.008$/GPa [Table I and Fig. 2(d)]. In the measured Raman spectra showing a one-peak feature,[12] the corresponding rate is $d\ln(\hbar\omega_a)/dP = 0.018$/GPa; so our phonon calculation seemingly underestimates the effect of pressure, even though our theoretical framework predicts the lattice constants of com-

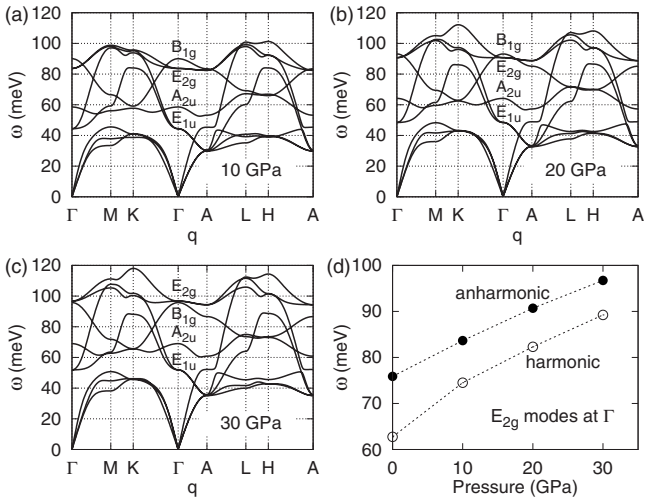

FIG. 2. Calculated phonon dispersions at (a) 10 GPa, (b) 20 GPa, (c) 30 GPa, and (d) calculated E_{2g} frequencies at Γ. In (a)–(c), anharmonicity is included in the dispersions. In (d), filled and empty circles are anharmonic and harmonic frequencies, respectively. The dotted lines are guides for the eyes.

pressed MgB_2 very well. Since the measured Raman spectrum may change in spectral shape under pressure,[13,14] the Green's function method might be appropriate to describe more correctly the E_{2g} phonons which are strongly interacting with the electrons. A model of this kind is beyond the scope of our present work, so we use our frozen-phonon calculations although it may reduce the effect of pressure on T_c.

We obtained the isotropically averaged electron-phonon coupling constant $\lambda=2\int d\omega\alpha^2F(\omega)/\omega$ from the calculated electronic and phononic structures and electron-phonon interaction at each pressure. The obtained coupling constant λ decreases with pressure, as shown in Fig. 3(a), and this is consistent with the decrease of $N(E_F)$ and hardening of E_{2g} phonons. At 30 GPa, λ decreases by 23%.

Figure 3(b) shows the superconducting transition temperature T_c obtained from the fully anisotropic Eliashberg equations at each pressure. The anisotropic Eliashberg equations at imaginary frequencies are[43,44]

$$Z(\mathbf{k},i\omega_n) = 1 + f_n s_n \sum_{\mathbf{k}'n'} W_{\mathbf{k}'}\lambda(\mathbf{k},\mathbf{k}',n-n') \times \frac{\omega_{n'}}{\sqrt{\omega_{n'}^2 + \Delta(\mathbf{k}',i\omega_{n'})^2}}, \quad (1)$$

$$Z(\mathbf{k},i\omega_n)\Delta(\mathbf{k},i\omega_n) = \pi T \sum_{\mathbf{k}'n'} W_{\mathbf{k}'}[\lambda(\mathbf{k},\mathbf{k}',n-n') - \mu^*(\omega_c)] \times \frac{\Delta(\mathbf{k}',i\omega_{n'})}{\sqrt{\omega_{n'}^2 + \Delta(\mathbf{k}',i\omega_{n'})^2}}, \quad (2)$$

where $\omega_n=(2n+1)\pi T$ is the fermionic Matsubara frequency at temperature T, $Z(\mathbf{k},i\omega_n)$ and $\Delta(\mathbf{k},i\omega_n)$ are the momentum-dependent renormalization function and the gap function, respectively, and $\lambda(\mathbf{k},\mathbf{k}',n)$ represents the momentum-dependent electron-phonon interaction. Definitions of symbols and details of the numerical method are described in Refs. 3, 43, and 44. Here, we assumed that the Coulomb pseudopotential μ^* does not vary with pressure[45] and used $\mu^*(\omega_c)=0.12$ for the cut-off frequency $\omega_c=0.5$ eV. We also assumed that μ^* is isotropic since its momentum dependence is not as significant as that of the electron-phonon interaction.[46–48] At 30 GPa, the calculated T_c is 24 K, which is 15 K lower than that of the uncompressed case, so we have $dT_c/dP \simeq -0.5$ K/GPa. This value does not deviate much from the wide range of the measured values, but it is about one half of −1.1 K/GPa which is suggested to be the intrinsic value under hydrostatic pressure experimentally. This discrepancy may originate from the anomalous effect of pressure on E_{2g} phonons, which is observed in the Raman spectra but not captured accurately in our phonon calculation.

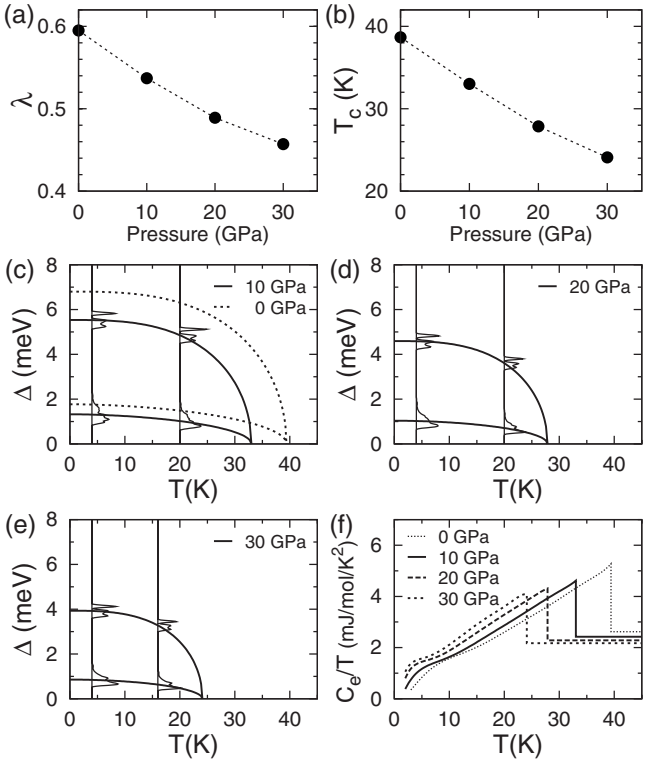

FIG. 3. Calculated electron-phonon interaction and superconducting properties of compressed MgB_2: (a) the averaged electron-phonon coupling strength λ, (b) the calculated T_c from the full anisotropic Eliashberg equations, (c)–(e) superconducting energy gaps at 10, 20, and 30 GPa, respectively, and (f) electronic contribution to the specific heat divided by temperature C_e/T. Dotted lines in (a) and (b) are guides for the eyes. In (c)–(e), the distributions of the superconducting energy gap are drawn vertically at 4 and 20 K and solid lines are curves of the form $\Delta(T) = \Delta(0)\sqrt{1-(T/T_c)^p}$ fit to $\Delta_\sigma(T)$ and $\Delta_\pi(T)$, respectively, using $\Delta(0)$ and p as fitting parameters. Dotted lines in (c) and the thin dotted line in (f) drawn for comparison are the corresponding values at 0 GPa.

To analyze the low-temperature superconducting properties of compressed MgB_2, we calculated the Fermi-surface distribution of the superconducting energy gap at various temperatures and pressures [Figs. 3(c)–3(e)], and we also

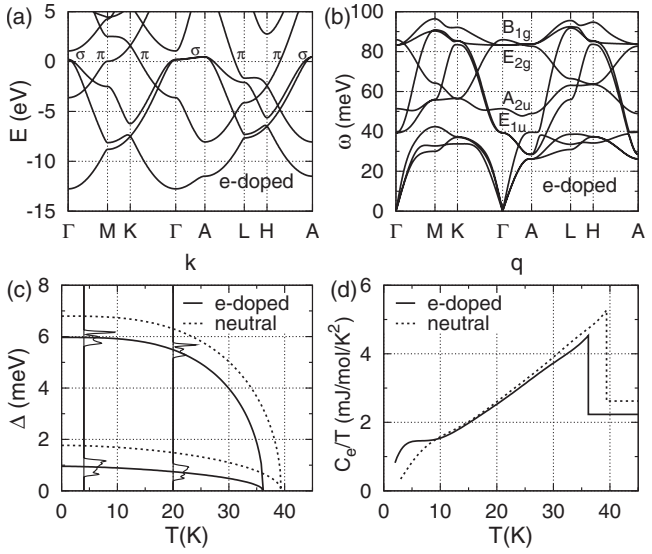

FIG. 4. Calculated electronic, vibrational, and superconducting properties of electron-doped MgB_2: (a) electronic band dispersions, (b) phonon dispersions, (c) superconducting energy gaps, and (d) electronic contribution to the specific heat divided by temperature. The doping concentration is 0.2 excess electron per unit cell, which corresponds to $Mg_{0.8}Al_{0.2}B_2$ or $Mg(B_{0.9}C_{0.1})_2$. In (c), the distributions of the superconducting energy gap are drawn vertically at 4 and 20 K and solid lines are curves of the form $\Delta(T) = \Delta(0)\sqrt{1-(T/T_c)^p}$ fit to $\Delta_\sigma(T)$ and $\Delta_\pi(T)$, respectively, using $\Delta(0)$ and p as fitting parameters. Dotted lines in (c) and the thin dotted line in (d) drawn for comparison are the corresponding values with no doping, which are the same as 0 GPa in Figs. 3(c) and 3(f).

obtained the electronic contribution C_e to the specific heat as a function of temperature and pressure [Fig. 3(f)]. The calculational methods for these superconducting properties are described in our previous publications.[4,43,44]

The distribution of the superconducting energy gap shown in Figs. 3(c)–3(e) indicates clearly that the multiple-gap nature persists at high pressure, even though T_c and the magnitudes of two gaps decrease substantially. Both the large gap and the small gap decrease with pressure in very similar rate to T_c so that $2\Delta_\sigma(0)/k_BT_c$ and $2\Delta_\pi(0)/k_BT_c$ are almost independent of pressure, as shown in Table I. At 30 GPa, the ratios are $2\Delta_\sigma(0)/k_BT_c=3.8$ and $2\Delta_\pi(0)/k_BT_c=0.83$, which are 95% and 75% of those at 0 GPa, respectively.

Since the averaged electron-phonon coupling strength λ decreases with pressure, the specific heat above T_c decreases. The height of the specific-heat jump in C_e/T at T_c also decreases, while the specific heat increases at very low temperature because of the decrease in the small superconducting energy gap Δ_π. At 30 GPa, the normal-state Sommerfeld coefficient $\gamma_N \equiv C_e/T$ decreases by 17% and the jump at T_c decreases by 28%. Because of the robust two-gap nature, the temperature dependence of the specific heat under pressure is still very different from a one-gap BCS model, although T_c is significantly reduced.

The effect of electron doping in MgB_2 is studied by introducing excess electrons in the first-principles calculations without changing the atomic structure. Figure 4 shows material properties and superconducting properties of electron-doped MgB_2 with 0.2 excess electrons per unit cell. In calculations for electronic and phononic structures, the total number of electrons in the unit cell is changed to 8.2 and then the system is made to be charge neutral by a compensating uniform background charge, while the lattice structure is fixed to the undoped case. The electron-doping concentration corresponds to $Mg_{0.8}Al_{0.2}B_2$ or $Mg(B_{0.9}C_{0.1})_2$; that is, 20% replacement of Mg or 10% of B, assuming total charge transfer.

In our calculation, the density of states at the Fermi energy $N(E_F)$ for 0.2 electron doping is 0.62 states/eV/unit cell which is reduced by 10% from 0.69 states/eV/unit cell of the undoped one. According to the theoretical result using the virtual-crystal approximation (VCA) for $Mg_{0.8}Al_{0.2}B_2$, the lattice constant a is reduced by 0.4%, c is reduced by 2.2%, and $N(E_F)$ is reduced by 11% to 0.64 states/eV/unit cell.[49] In the case of $Mg(B_{0.9}C_{0.1})_2$, density-functional calculations using supercells have shown that a is reduced by 1% while c is almost constant[50] and that $N(E_F)$ is reduced by 14%, with more reduction in the π bands than in the σ bands.[50] By comparing our results and the VCA results,[49] we note that the reduction of $N(E_F)$ with doping is not due to the change in the lattice constants but due to the increase in the number of electrons. Furthermore, if we estimate the effect of the volume change on $N(E_F)$ using the theoretical data for MgB_2 under pressure, the 3% volume reduction in the VCA work would correspond to a pressure of 5.5 GPa and would reduce $N(E_F)$ by 0.01 states/eV/unit cell. This is negligible compared with the effect of the electron doping. In our calculation $N(E_F)$ is reduced more in the π bands than in the σ bands, which is consistent with the results of the supercell calculations.[50]

Figure 4(b) shows the phonon dispersions in electron-doped MgB_2. Very noticeably, the frequency of the E_{2g} mode increases very rapidly with electron doping. Other modes are rather insensitive to the doping. With 0.2 more electrons, $\omega_{E_{2g}}$ increases by 10%. In Raman measurements with C-doped MgB_2, the peak position is shifted more than 30% with 10% carbon doping.[27] Compared with this Raman result, our calculation significantly underestimates the frequency shift of the E_{2g} modes again as in the cases for compressed structures. This may partly originate from the reduction in the unit-cell volume which is neglected in our calculation and/or from the anomalous behavior of E_{2g} modes observed in Raman spectra of doped samples as in the case of compression.

We obtain $T_c=36$ K for the electron-doped MgB_2 from the fully anisotropic Eliashberg equations, with the isotropic and constant value of $\mu^*(\omega_c)=0.12$ as in the case of pressure.[45] Thus, our theoretical value for the drop in T_c with the doping is 3 K, which is quite small compared with experimental values of drop in T_c for $Mg_{0.8}Al_{0.2}B_2$ and $Mg(B_{0.9}C_{0.1})_2$ samples that are in the range of 5–17 K.[15–20,22–27] As mentioned above, the 3% volume reduction in the VCA calculation[49] for $Mg_{0.8}Al_{0.2}B_2$, which is neglected in our calculation, corresponds to a pressure of 5.5 GPa in the case of compression. If we consider the volume reduction and the experimental value of $dT_c/dP \simeq -1.1$ K/GPa, we might have an additional drop of T_c by 6 K. Thus the volume reduction neglected in our calculation may partly

explain the difference of our theoretical value and the reported experimental ones. In addition, impurity scattering introduced by doping may decrease T_c further by driving the superconductivity of the material to the isotropic one,[3,34] possibly resulting in better agreement between theory and experiment.

Figures 4(c) and 4(d) show the superconducting energy gap and the specific heat in doped MgB_2. With electron doping, the small gap decreases much faster than the large gap, resulting in $\Delta_\sigma(0)=6.0$ meV and $\Delta_\pi(0)=0.96$ meV. Thus, the ratio $\Delta_\sigma(0)/\Delta_\pi(0)$ is changed significantly by doping. Compared with experimental results for $Mg_{0.8}Al_{0.2}B_2$ and $Mg(B_{0.9}C_{0.1})_2$, Δ_σ is overestimated and Δ_π is underestimated in our calculations. The overestimation of Δ_σ seems consistent with the small drop of T_c in our calculation; however, the underestimation of Δ_π does not look consistent, so it suggests again that perhaps impurity scattering plays a role, as mentioned above in comparing theoretical and experimental values of T_c. The impurity scattering is not considered in our present work but does exist in real samples. Since Δ_π is reduced significantly, the specific heat divided by temperature C_e/T is increased strongly at temperatures below 10 K [Fig. 4(d)].

To summarize, we have performed *ab initio* pseudopotential calculations for lattice parameters, electronic and phononic structures, and electron-phonon interactions in compressed and doped MgB_2 and obtained their superconducting properties from the fully anisotropic Eliashberg equations. Our results show a smaller reduction of T_c under pressure and doping than the experimental results. We find a robust two-gap nature for the case of compressed samples and a strong suppression of Δ_π in the case of electron doping.

This work was supported by the NSF under Grant No. DMR07-05941, by the Director, Office of Science, Office of Basic Energy Sciences, Materials Sciences and Engineering Division, U.S. Department of Energy under Contract No. DE-AC02-05CH11231, by the KRF (Grant No. KRF-2007-314-C00075), and by the KOSEF under Grant No. R01-2007-000-20922-0. Computational resources have been provided by NSF through TeraGrid resources at SDSC, DOE at Lawrence Berkeley National Laboratory's NERSC facility, and KISTI Supercomputing Center (Project No. KSC-2007-S00-1011).

*h.j.choi@yonsei.ac.kr

[1] J. Nagamatsu, N. Nakagawa, T. Muranaka, Y. Zenitani, and J. Akimitsu, Nature (London) **410**, 63 (2001).
[2] A. Y. Liu, I. I. Mazin, and J. Kortus, Phys. Rev. Lett. **87**, 087005 (2001).
[3] H. J. Choi, D. Roundy, H. Sun, M. L. Cohen, and S. G. Louie, Phys. Rev. B **66**, 020513(R) (2002).
[4] H. J. Choi, D. Roundy, H. Sun, M. L. Cohen, and S. G. Louie, Nature (London) **418**, 758 (2002).
[5] C. Buzea and T. Yamashita, Supercond. Sci. Technol. **14**, R115 (2001), and references therein.
[6] M. Monteverde, M. Núñez-Regueiro, N. Rogado, K. A. Regan, M. A. Hayward, T. He, S. M. Loureiro, and R. J. Cava, Science **292**, 75 (2001).
[7] E. Saito, T. Taknenobu, T. Ito, Y. Iwasa, K. Prassides, and T. Arima, J. Phys.: Condens. Matter **13**, L267 (2001).
[8] V. G. Tissen, M. V. Nefedova, N. N. Kolesnikov, and M. P. Kulakov, Physica C **363**, 194 (2001).
[9] T. Masui, K. Yoshida, S. Lee, A. Yamamoto, and S. Tajima, Phys. Rev. B **65**, 214513 (2002).
[10] S. Deemyad, T. Tomita, J. J. Hamlin, B. R. Beckett, J. S. Schilling, D. G. Hinks, J. D. Jorgensen, S. Lee, and S. Tajima, Physica C **385**, 105 (2003).
[11] T. Tomita, J. J. Hamlin, J. S. Schilling, D. G. Hinks, and J. D. Jorgensen, Phys. Rev. B **64**, 092505 (2001).
[12] A. F. Goncharov, V. V. Struzhkin, E. Gregoryanz, J. Hu, R. J. Hemley, H. K. Mao, G. Lapertot, S. L. Budko, and P. C. Canfield, Phys. Rev. B **64**, 100509(R) (2001).
[13] K. Kunc, I. Loa, K. Syassen, R. K. Kremer, and K. Ahn, J. Phys.: Condens. Matter **13**, 9945 (2001).
[14] I. Loa, K. Kunc, and K. Syassen, High Press. Res. **23**, 129 (2003).
[15] M. Putti, M. Affronte, P. Manfrinetti, and A. Palenzona, Phys. Rev. B **68**, 094514 (2003).
[16] J. Q. Li, L. Li, F. M. Liu, C. Dong, J. Y. Xiang, and Z. X. Zhao, Phys. Rev. B **65**, 132505 (2002).
[17] A. Bianconi, S. Agrestini, D. Di Castro, G. Campi, G. Zangari, N. L. Saini, A. Saccone, S. De Negri, M. Giovannini, G. Profeta, A. Continenza, G. Satta, S. Massidda, A. Cassetta, A. Pifferi, and M. Colapietro, Phys. Rev. B **65**, 174515 (2002).
[18] B. Renker, K. B. Bohnen, R. Heid, D. Ernst, H. Schober, M. Koza, P. Adelmann, P. Schweiss, and T. Wolf, Phys. Rev. Lett. **88**, 067001 (2002).
[19] P. Szabo, P. Samuely, Z. Pribulova, M. Angst, S. Bud'ko, P. C. Canfield, and J. Marcus, Phys. Rev. B **75**, 144507 (2007).
[20] P. Postorino, A. Congeduti, P. Dore, A. Nucara, A. Bianconi, D. Di Castro, S. De Negri, and A. Saccone, Phys. Rev. B **65**, 020507(R) (2001).
[21] L. D. Cooley, A. J. Zambano, A. R. Moodenbaugh, R. F. Klie, J.-C. Zheng, and Y. Zhu, Phys. Rev. Lett. **95**, 267002 (2005).
[22] S. M. Kazakov, R. Puzniak, K. Rogacki, A. V. Mironov, N. D. Zhigadlo, J. Jun, Ch. Soltmann, B. Batlogg, and J. Karpinski, Phys. Rev. B **71**, 024533 (2005).
[23] A. Bharathi, S. Jemima Balaselvi, S. Kalavathi, G. L. N. Reddy, V. S. Sastry, Y. Hariharan, and T. S. Radhakrishnan, Physica C **370**, 211 (2002).
[24] H. Schmidt, K. E. Gray, D. G. Hinks, J. F. Zasadzinski, M. Avdeev, J. D. Jorgensen, and J. C. Burley, Phys. Rev. B **68**, 060508(R) (2003).
[25] Z. Hol'anová, P. Szabó, P. Samuely, R. H. T. Wilke, S. L. Bud'ko, and P. C. Canfield, Phys. Rev. B **70**, 064520 (2004).
[26] S. Tsuda, T. Yokoya, T. Kiss, T. Shimojima, S. Shin, T. Togashi, S. Watanabe, C. Zhang, C. T. Chen, S. Lee, H. Uchiyama, S. Tajima, N. Nakai, and K. Machida, Phys. Rev. B **72**, 064527

(2005).
[27] T. Masui, S. Lee, and S. Tajima, Phys. Rev. B **70**, 024504 (2004).
[28] I. Loa and K. Syassen, Solid State Commun. **118**, 279 (2001).
[29] X. J. Chen, H. Zhang, and H.-U. Habermeier, Phys. Rev. B **65**, 144514 (2002).
[30] G. Profeta, A. Continenza, and S. Massidda, Phys. Rev. B **68**, 144508 (2003).
[31] R. Ma, M. Liu, Y. G. Wang, and Y. H. Yang, Phys. Status Solidi B **244**, 1082 (2007).
[32] G. A. Ummarino, R. S. Gonnelli, S. Massidda, and A. Bianconi, Physica C **407**, 121 (2004).
[33] G. A. Ummarino, Physica C **423**, 96 (2005).
[34] J. Kortus, O. V. Dolgov, R. K. Kremer, and A. A. Golubov, Phys. Rev. Lett. **94**, 027002 (2005).
[35] G. M. Eliashberg, Zh. Eksp. Teor. Fiz. **38**, 966 (1960) [Sov. Phys. JETP **11**, 696 (1960)].
[36] P. B. Allen and B. Mitrović, in *Solid State Physics*, edited by H. Ehrenreich, F. Seitz, and D. Turnbull (Academic, New York, 1982), Vol. 37, p. 1, and references therein.
[37] N. Troullier and J. L. Martins, Phys. Rev. B **43**, 1993 (1991).
[38] J. Ihm, A. Zunger, and M. L. Cohen, J. Phys. C **12**, 4409 (1979).
[39] P. K. Lam and M. L. Cohen, Phys. Rev. B **25**, 6139 (1982).
[40] M. M. Dacorogna, M. L. Cohen, and P. K. Lam, Phys. Rev. Lett. **55**, 837 (1985).
[41] P. Bordet, M. Mezouar, M. Núñez-Regueiro, M. Monteverde, M. D. Núñez-Regueiro, N. Rogado, K. A. Regan, M. A. Hayward, T. He, S. M. Loureiro, and R. J. Cava, Phys. Rev. B **64**, 172502 (2001).
[42] T. Vogt, G. Schneider, J. A. Hriljac, G. Yang, and J. S. Abell, Phys. Rev. B **63**, 220505(R) (2001).
[43] H. J. Choi, M. L. Cohen, and S. G. Louie, Physica C **385**, 66 (2003).
[44] H. J. Choi, M. L. Cohen, and S. G. Louie, Phys. Rev. B **73**, 104520 (2006).
[45] The assumption of a constant μ^* in our calculation independent of applied pressure or doping is a reasonable approximation because of the relatively weak dependence of μ^* on $N(E_F)$ for this range of densities.
[46] C.-Y. Moon, Y.-H. Kim, and K. J. Chang, Phys. Rev. B **70**, 104522 (2004).
[47] I. I. Mazin, O. K. Andersen, O. Jepsen, A. A. Golubov, O. V. Dolgov, and J. Kortus, Phys. Rev. B **69**, 056501 (2004).
[48] H. J. Choi, D. Roundy, H. Sun, M. L. Cohen, and S. G. Louie, Phys. Rev. B **69**, 056502 (2004).
[49] O. de la Peña, A. Aguayo, and R. de Coss, Phys. Rev. B **66**, 012511 (2002).
[50] A. H. Moudden, J. Phys. Chem. Solids **67**, 115 (2006).